

Extended Organic–Inorganic Hybrids Based on Dawson and Double-Dawson-Type Polyoxometalates

Zhiming Zhang, Yangguang Li,* Yonghui Wang, Yanfei Qi, and Enbo Wang*

Key Laboratory of Polyoxometalate Science of Ministry of Education, Department of Chemistry, Northeast Normal University, Renmin Street No. 5268, Changchun, Jilin 130024, People's Republic of China

Received March 18, 2008

The reaction between $K_{12}[H_2P_2W_{12}O_{48}]$ and $CuCl_2$ in a NaCl aqueous solution assisted with organoamines (1,2-ethylenediamine (en), 1,6-hexamethylene diamine (hn), or both) leads to the isolation of three compounds: $K_4Na_{10}[\alpha_1-CuP_2W_{17}O_{60}(OH)]_2 \cdot \sim 58H_2O$ (**1**), $Na_2[H_2en][H_2hn]_{0.5}[Cu(en)_2]_{4.5}[\alpha_1-CuP_2W_{17}O_{60}(OH)]_2 \cdot \sim 43H_2O$ (**2**), and $Na_3[H_2hn]_{2.5}[\alpha_1-P_2W_{17}O_{60}Cu(OH)_2] \cdot \sim 14H_2O$ (**3**). The polyoxoanion $[\alpha_1-CuP_2W_{17}O_{60}(OH)]_2^{14-}$ in **1** and **2** exhibits a double-Dawson-type polyoxoanion that consists of two α_1 -type mono-Cu-substituted Wells–Dawson anions, which can be synthesized by both the conventional aqueous solution method and the hydrothermal technique. Furthermore, the double-Dawson-type polyoxoanions in **2** are linked by the $[Cu(en)_2]^{2+}$ bridges to form 2-D networks, which are further packed into a 3-D supramolecular porous framework via extensive hydrogen bonding interactions, exhibiting two types of tunnels (A and B). Compound **3** possesses a 3-D supramolecular framework with 1-D tunnels constructed from the α_1 -type mono-Cu-substituted Wells–Dawson anion. The magnetic studies of compounds **1** and **2** indicate that weak antiferromagnetic interactions exist in these two compounds.

Introduction

Because of their controllable shape and size, their highly negative charges, and their oxo-enriched surfaces, polyoxometalates (POMs) have attracted great interest in constructing high-dimensional frameworks, which may possess a series of potential applications in catalysis, electrical conductivity, gas storage, ion exchange, and biological chemistry.^{1,2} In

the past decades, a series of inorganic–organic hybrids based on POMs and various metal–organic complexes has been reported in which the metal–organic coordination complexes provide charge compensation and become a part of the inorganic POM framework. However, the polyoxoanions in these extended organic–inorganic hybrid materials are mostly limited to polyoxomolybdates and polyoxovanadates, such as Mo_6 ,³ Mo_8 ,⁴ Mo_{12} ,⁵ V_{18} ,⁶ and the mixed-Mo/V⁷ clusters. Recently, the synthesis of the extended hybrid solid-

* To whom correspondence should be addressed. E-mail: wangeb889@nenu.edu.cn (E.W.), liyg658@nenu.edu.cn (Y.L.). Fax: +86-431-85098787.

- (1) (a) Pope, M. T. *Heteropoly and Isopoly Oxometalates*; Springer: Berlin, 1983. (b) Anderson, J. S. *Nature* **1937**, *140*, 850. (c) Hill, C. L. *Chem. Rev.* **1998**, *98*, 1. (d) Xu, B.; Peng, Z.; Wei, Y.; Powell, D. R. *Chem. Commun.* **2003**, 2562. (e) Baker, L. C. W.; Glick, D. C. *Chem. Rev.* **1998**, *98*, 3. (f) Müller, A.; Shah, S. Q. N.; Bögge, H.; Schmidtman, M. *Nature* **1999**, *397*, 48. (g) Fukaya, K.; Yamase, T. *Angew. Chem., Int. Ed.* **2003**, *42*, 654. (h) Coronado, E.; Gómez-García, C. J. *Chem. Rev.* **1998**, *98*, 273. (i) Lu, C.-Z.; Wu, C.-D.; Zhuang, H.-H.; Huang, J.-S. *Chem. Mater.* **2002**, *14*, 2649. (j) Li, Q.; Wei, Y.; Hao, J.; Zhu, Y.; Wang, L. *J. Am. Chem. Soc.* **2007**, *129*, 5810. (k) Long, D. L.; Burkholder, E.; Cronin, L. *Chem. Soc. Rev.* **2007**, *36*, 105.
- (2) (a) An, H. Y.; Wang, E. B.; Xiao, D. R.; Li, Y. G.; Su, Z. M.; Xu, L. *Angew. Chem., Int. Ed.* **2006**, *45*, 904. (b) Wei, M.; He, C.; Hua, W.; Duan, C.; Li, S.; Meng, Q. *J. Am. Chem. Soc.* **2006**, *128*, 13318. (c) Uehara, K.; Nakao, H.; Kawamoto, R.; Hikichi, S.; Mizuno, N. *Inorg. Chem.* **2006**, *45*, 9448. (d) Ishii, Y.; Takenaka, Y.; Konishi, K. *Angew. Chem., Int. Ed.* **2004**, *43*, 2702. (e) Knaust, J. M.; Inman, C.; Keller, S. W. *Chem. Commun.* **2004**, 492. (f) Kawamoto, R.; Uchida, S.; Mizuno, N. *J. Am. Chem. Soc.* **2005**, *127*, 10560.

- (3) (a) Chang, W.-J.; Jiang, Y.-C.; Wang, S.-L.; Lii, K.-H. *Inorg. Chem.* **2006**, *45*, 6586. (b) Shivaiah, V.; Reddy, P. V. N.; Cronin, L.; Das, S. K. *J. Chem. Soc., Dalton Trans.* **2002**, 3781. (c) Xia, Y.; Wu, P. F.; Wei, Y. G.; Wang, Y.; Guo, H. Y. *Cryst. Growth Des.* **2006**, *6*, 253.
- (4) (a) Zapf, P. J.; Warren, C. J.; Haushalter, R. C.; Zubieta, J. *J. Chem. Soc., Chem. Commun.* **1997**, 1543. (b) Jin, H.; Qi, Y.-F.; Wang, E.-B.; Li, Y.-G.; Wang, X.-L.; Qin, C.; Chang, S. *Cryst. Growth Des.* **2006**, *6*, 2693. (c) Hagman, D.; Zubieta, C.; Haushalter, R. C.; Zubieta, J. *Angew. Chem., Int. Ed. Engl.* **1997**, *36*, 873. (d) Wu, C.-D.; Lu, C.-Z.; Zhuang, H.-H.; Huang, J.-S. *Inorg. Chem.* **2002**, *41*, 5636. (e) Pavani, K.; Lofland, S. E.; Ramanujachary, K. V.; Ramanan, A. *Eur. J. Inorg. Chem.* **2007**, 568. (f) Li, S.-L.; Lan, Y.-Q.; Ma, J.-F.; Yang, J.; Wang, X.-H.; Su, Z.-M. *Inorg. Chem.* **2007**, *46*, 8283.
- (5) (a) Wang, X.-L.; Qin, C.; Wang, E.-B.; Su, Z.-M.; Li, Y.-G.; Xu, L. *Angew. Chem., Int. Ed.* **2006**, *45*, 7411. (b) Lei, C.; Mao, J.-G.; Sun, Y.-Q.; Song, J.-L. *Inorg. Chem.* **2004**, *43*, 1964. (c) Shi, Z.; Peng, J.; Gómez-García, C. J.; Benmansour, S.; Gu, X. *J. Solid State Chem.* **2006**, *179*, 253. (d) Dolbecq, A.; Mialane, P.; Lisnard, L.; Marrot, J.; Sécheresse, F. *Chem.—Eur. J.* **2003**, *9*, 2914.

state materials based on polyoxotungstate clusters has attracted considerable attention, and examples of these high-dimensional materials are mostly based on Keggin-type anions or the smaller POM clusters.⁸ Compared with these well-known POMs, such as Keggin-, Anderson-, and Lindqvist-type POMs, the Wells–Dawson type anions possess a larger molecular size with 18 terminal O atoms and 36 μ_2 -O atoms, which offers smarter potential coordination sites to link metal–organic units and to make the formation of a high-dimensional framework easier. Polyoxometalate chemists are eager to extend the Dawson-POM-based coordination polymers family; however, the high-dimensional materials based on the Dawson polyoxoanions were rarely reported⁹ possibly because the large size of these POMs decreases the electron density or the oxygen coordination ability on their surfaces.^{10f}

In this field, an important fact is that the greater the charge density on the surface oxygen atoms of POMs the more metal–organic complex units coordinated to the POMs. As a result, such highly negative polyoxoanions may be easily linked by more bridging fragments to form high-dimensional materials. During the preparation, two strategies have been exploited to increase the surface charge density and to activate the surface oxygen atoms of polyoxoanions:¹⁰ (a) decreasing the oxidation states of metal centers in POMs, for example, from $W(\text{Mo})^{\text{VI}}$ to $W(\text{Mo})^{\text{V}}$, with strong reducing reagents or (b) substituting the W^{VI} metal centers with other metal centers, such as V^{IV} or TM^{II} . As for the large POMs, Dawson-type polyoxotungstate is an ideal candidate because it is structurally stable and is chemically easily available. Until now, several extended frameworks based on the Dawson-type polyoxoanions and metal–organic complexes have been reported,^{9,11} such as $[(\text{Ce}(\text{DMF})_4(\text{H}_2\text{O})_3)(\text{Ce}(\text{DMF})_4(\text{H}_2\text{O})_4)(\text{P}_2\text{W}_{18}\text{O}_{62})]$,^{11a} $[(\text{Gd}(\text{DMF})_6)(\text{Gd}(\text{DMF})_7)-(\text{P}_2\text{W}_{18}\text{O}_{62})]$,^{11b} $[(\text{Cu}_2(2,4\text{-Hbpy})_4)\text{Mo}_{18}\text{As}_2\text{O}_{62}]$,^{11c} $[\text{Zn}(\text{phen})_2(\text{H}_2\text{O})_2][(\text{Zn}(\text{phen})_2)(\text{Zn}(\text{phen})_2(\text{H}_2\text{O}))(\text{P}_2\text{W}_{18}\text{O}_{62})]$,^{11f} $[\text{Cd}(\text{phen})_2(\text{H}_2\text{O})_2][(\text{Cd}(\text{phen})_2)(\text{Cd}(\text{phen})(\text{H}_2\text{O})_3)(\text{P}_2\text{W}_{18}\text{O}_{62})]$,^{11f} $[\text{Cu}(\text{en})_2(\text{OH})_2]_2[\text{H}_2\text{en}][(\text{Cu}(\text{en})_2)\text{P}_2\text{CuW}_{17}\text{O}_{61}]$,^{9a} $[\text{Cu}(\text{en})_2(\text{OH})_2]_2[\text{Cu}(\text{en})_2]_{0.5}[\text{H}_2\text{en}]_{0.5}[(\text{Cu}(\text{en})_2)\text{P}_2\text{CuW}_{17}\text{O}_{61}]$,^{9a} and $(\text{H}_2\text{en})_{0.5}\text{H}[\text{Cu}(\text{en})_2(\text{H}_2\text{O})]_2[(\text{Cu}(\text{en})_2)(\alpha_1\text{-P}_2\text{W}_{17}\text{CuO}_{61})]$.^{11d} In this field, we have also obtained several 1-D and 2-D compounds based on Wells–Dawson POMs.^{11e,g} However, the composition of the Dawson-type anion has rarely been

adjusted in all of the above-reported Dawson-based extended frameworks.¹¹ Therefore, the exploration of feasible synthetic routes to adjust the composition of Wells–Dawson-type anions and to increase the surface charge density and to activate the surface oxygen atoms of such polyoxoanions is still a challenging issue. In this work, we choose the very lacunary anion $[\text{H}_2\text{P}_2\text{W}_{12}\text{O}_{48}]^{12-}$ (abbreviated as P_2W_{12}) as the starting material to capture more low-valence TM cations so as to make the TM-substituted Dawson-type polyoxoanions with a higher surface charge density and a larger size simultaneously. Herein, we reported three POM-based hybrid compounds in this subfamily: $\text{K}_2\text{Na}_{10}[\alpha_1\text{-CuP}_2\text{W}_{17}\text{O}_{60}(\text{OH})_2] \cdot \sim 58\text{H}_2\text{O}$ (**1**), $\text{Na}_2[\text{H}_2\text{en}][\text{H}_2\text{hn}]_{0.5}[\text{Cu}(\text{en})_2]_{4.5}[\alpha_1\text{-CuP}_2\text{W}_{17}\text{O}_{60}(\text{OH})_2] \cdot \sim 43\text{H}_2\text{O}$ (**2**), and $\text{Na}_3[\text{H}_2\text{hn}]_{2.5}[\text{P}_2\text{W}_{17}\text{O}_{60}\text{Cu}(\text{OH})_2] \cdot \sim 14\text{H}_2\text{O}$ (**3**) (en is 1,2-ethylenediamine; hn is 1,6-hexamethylene diamine). Compound **1** contains a double-Dawson-type polyoxoanion (DDTP) that is rarely reported in POM chemistry.^{15f} Compound **2** represents the first 2-D organic–inorganic hybrid network based on such DDTP building blocks. Compound **3** possesses a 3-D hybrid supramolecular framework with 1-D tunnels that are constructed from the half-unit of the DDTP and hn cations.

Experimental Section

Materials and Methods. All chemicals were commercially purchased and were used without further purification. $\text{K}_{12}[\text{H}_2\text{P}_2\text{W}_{12}\text{O}_{48}] \cdot \sim 24\text{H}_2\text{O}$ was synthesized according to the literature¹² and was characterized by the IR spectrum. Elemental analyses (H, C, and N) were performed on a Perkin-Elmer 2400 CHN elemental analyzer; P, W, Cu, K, and Na were analyzed on a Plasma-Spec (I) ICP atomic emission spectrometer. Infrared spectra were recorded in the range of 400–4000 cm^{-1} on an Alpha Centaur FT/IR spectrophotometer using KBr pellets. Magnetic susceptibility measurements of compounds **1** and **2** were performed on a Quantum Design SQUID magnetometer (MPMS-XL). Direct current measurements were conducted from 1.8 to 300 K at 0.1 T. The measurements were performed on polycrystalline samples. Experimental data were corrected for the sample holder and for the sample's diamagnetic contribution calculated from Pascal constants.¹³

- (6) (a) Khan, M. I.; Yohannes, E.; Doedens, R. *J. Angew. Chem., Int. Ed.* **1999**, *38*, 1292. (b) Yang, W.; Lu, C.; Zhang, Q.; Chen, S.; Zhan, X.; Liu, J. *Inorg. Chem.* **2003**, *42*, 7309.
- (7) (a) Liu, C.-M.; Zhang, D.-Q.; Xiong, M.; Zhu, D.-B. *Chem. Commun.* **2002**, 1416. (b) Duan, L.-M.; Pan, C.-L.; Xu, J.-Q.; Cui, X.-B.; Xie, F.-T.; Wang, T.-G. *Eur. J. Inorg. Chem.* **2003**, 2578.
- (8) (a) Lisnard, L.; Dolbecq, A.; Mialane, P.; Marrot, J.; Codjovi, E.; Sécheresse, F. *Dalton Trans.* **2005**, 3913. (b) Fan, L. L.; Xiao, D. R.; Wang, E. B.; Li, Y. G.; Su, Z. M.; Wang, X. L.; Liu, J. *Cryst. Growth Des.* **2007**, *7*, 592. (c) Zheng, P.-Q.; Ren, Y.-P.; Long, L.-S.; Huang, R.-B.; Zheng, L.-S. *Inorg. Chem.* **2005**, *44*, 1190. (d) Ren, Y.-P.; Kong, X.-J.; Hu, X.-Y.; Sun, M.; Long, L.-S.; Huang, R.-B.; Zheng, L.-S. *Inorg. Chem.* **2006**, *45*, 4016. (e) Kong, X.-J.; Ren, Y.-P.; Zheng, P.-Q.; Long, Y.-X.; Long, L.-S.; Huang, R.-B.; Zheng, L.-S. *Inorg. Chem.* **2006**, *45*, 10702. (f) Reinoso, S.; Vitoria, P.; San Felices, L.; Montero, A.; Lezama, L.; Gutiérrez-Zorrilla, J. M. *Inorg. Chem.* **2007**, *46*, 1237.
- (9) (a) Yan, B.; Xu, Y.; Bu, X.; Goh, N. K.; Chia, L. S.; Stucky, G. D. *J. Chem. Soc., Dalton Trans.* **2001**, 2009. (b) Tian, A.-x.; Ying, J.; Peng, J.; Sha, J.-q.; Han, Z.-g.; Ma, J.-f.; Su, Z.-m.; Hu, N.-h.; Jia, H.-q. *Inorg. Chem.* **2008**, *47*, 3274.

- (10) (a) San Felices, L.; Vitoria, P.; Gutiérrez-Zorrilla, J. M.; Lezama, L.; Reinoso, S. *Inorg. Chem.* **2006**, *45*, 7748. (b) Gouzerh, P.; Villanneau, R.; Delmont, R.; Proust, A. *Chem.–Eur. J.* **2000**, *6*, 1184. (c) *Polyoxometalate Chemistry: From Topology via Self-Assembly to Applications*; Pope, M. T., Müller, A., Eds.; Kluwer: Dordrecht, The Netherlands, 2001. (d) *Polyoxometalate Chemistry for Nano-Composite Design*; Yamase, T., Pope, M. T., Eds.; Kluwer: Dordrecht, The Netherlands, 2002; (e) Coronado, E.; Giménez-Saiz, C.; Gómez-García, C. J. *Coord. Chem. Rev.* **2005**, *249*, 1776. (f) Yu, K.; Li, Y.-G.; Zhou, B.-B.; Su, Z.-H.; Zhao, Z.-F.; Zhang, Y.-N. *Eur. J. Inorg. Chem.* **2007**, 5662. (g) Holscher, M.; Englert, U.; Zibrowius, B.; Holderich, W. F. *Angew. Chem., Int. Ed. Engl.* **1994**, *33*, 2491.
- (11) (a) Niu, J. Y.; Guo, D. J.; Wang, J. P.; Zhao, J. W. *Cryst. Growth Des.* **2004**, *4*, 241. (b) Niu, J.; Guo, D.; Zhao, J.; Wang, J. *Chem. J. Chem.* **2004**, *28*, 980. (c) Soumahoro, T.; Burkholder, E.; Ouellette, W.; Zubietta, J. *Inorg. Chim. Acta* **2005**, *358*, 606. (d) Zhao, J.-W.; Zheng, S.-T.; Liu, W.; Yang, G.-Y. *J. Solid State Chem.* **2008**, *181*, 637. (e) Lu, Y.; Xu, Y.; Li, Y.; Wang, E.; Xu, X.; Ma, Y. *Inorg. Chem.* **2006**, *45*, 2055. (f) Tian, A. X.; Han, Z. B.; Peng, J.; Dong, B. X.; Sha, J. Q.; Li, B. *J. Mol. Struct.* **2007**, *832*, 117. (g) Jin, H.; Qi, Y. F.; Xiao, D. R.; Wang, X. L.; Chang, S.; Wang, E. B. *J. Mol. Struct.* **2007**, *837*, 23.
- (12) Contant, R.; Tézé, A. *Inorg. Chem.* **1985**, *24*, 4610.
- (13) *Theory and Applications of Molecular Paramagnetism*; Boudreaux, E. A., Mulay, L. N., Eds.; Wiley: New York, 1976.

Table 1. Crystal Data and Structure Refinement for Compounds 1–3

	1	2	3
empirical formula	H ₁₁₈ Cu ₂ K ₄ Na ₁₀ O ₁₈₀ P ₄ W ₃₄	C ₂₃ H ₁₇₉ Cu _{6.5} N ₂₁ Na ₂ O ₁₆₅ P ₄ W ₃₄	C ₁₅ H ₇₅ CuN ₅ Na ₃ O ₇₆ P ₂ W ₁₇
mol wt	9887.11	10 224.64	4861.70
λ (Å)	0.71073	0.71073	0.71073
<i>T</i> (K)	150(2)	150(2)	150(2)
cryst dimensions (mm ³)	0.17 × 0.15 × 0.14	0.20 × 0.18 × 0.15	0.20 × 0.17 × 0.13
cryst syst	monoclinic	triclinic	triclinic
space group	<i>C2/c</i>	<i>P</i> $\bar{1}$	<i>P</i> $\bar{1}$
<i>a</i> (Å)	43.782(9)	15.9675(8)	12.856(3)
<i>b</i> (Å)	12.338(3)	22.8146(12)	15.712(3)
<i>c</i> (Å)	29.651(6)	27.4263(14)	22.730(5)
α (deg)	90	103.7760(10)	84.01(3)
β (deg)	101.51	103.6730(10)	89.52(3)
γ (deg)	90	106.5970(10)	68.41(3)
<i>V</i> (Å ³)	15 695(5)	8788.1(8)	4243.9(15)
<i>Z</i>	4	2	2
<i>D_c</i> (mg·m ⁻³)	4.184	3.864	3.805
μ (mm ⁻¹)	25.375	23.079	23.344
<i>F</i> (000)	17 512	9141	4316
θ range(deg)	3.00–25.00	2.47–25.00	3.02–25.00
data (<i>R_{int}</i>)/restraints/parameters	13 611 (0.1673)/162/903	30 785 (0.0445)/400/2039	14 626 (0.1188)/211/897
<i>R</i> ₁ (<i>I</i> > 2 σ (<i>I</i>)) ^a	0.0678	0.0546	0.0742
w <i>R</i> ₂ (all data) ^b	0.1288	0.1340	0.1484
GOF on <i>F</i> ²	1.003	1.065	1.026

$$^a R_1 = \sum |F_o| - |F_c| / \sum |F_o| \quad ^b wR_2 = \sum [w(F_o^2 - F_c^2)^2] / \sum [w(F_o^2)^2]^{1/2}$$

Synthesis of Compound 1. CuCl₂·2H₂O (0.4 g, 2.35 mmol) was dissolved in 100 mL of 1 M LiCl containing 0.5 mL of glacial acetic acid (HAc). Then, freshly prepared K₁₂[H₂P₂W₁₂O₄₈]·~24H₂O (1.0 g, 0.25 mmol) and NaCl (0.1 g, 1.71 mmol) were added to this solution with vigorous stirring and were further stirred for 8 h. The resulting solution was filtered, and the filtrate was kept at room temperature for slow evaporation. Light-blue block crystals of **1** were isolated after 4 weeks (in 32% yield, based on P). Anal. Calcd for **1**: K, 1.58; Na, 2.33; Cu, 1.29; P, 1.25; W, 63.2. Found: K, 1.39; Na, 2.41; Cu, 1.35; P, 1.01; W, 62.9. IR (KBr pellet) $\bar{\nu}_{\max}$ (cm⁻¹): 1125 (w), 1084 (w), 952 (s), 903 (s), 801 (s), 519 (w).

Synthesis of Compound 2. K₁₂[H₂P₂W₁₂O₄₈]·~24H₂O (0.3 g, 0.076 mmol), 1 M CuCl₂ aqueous solution (0.75 mL, 0.75 mmol), en (0.15 mL, 2.24 mmol), hn (0.05 mL, 0.488 mmol), and NaCl (0.05 g, 0.86 mmol) were dissolved in 9 mL of distilled water. The mixture was stirred for 0.5 h and was transferred to a Teflon-lined stainless-steel autoclave (15 mL). The Teflon-lined stainless-steel autoclave was heated to 160 °C within 45 min, was kept at 160 °C for 15 days, and was then cooled to room temperature at a rate of 10 °C/h. Brown blocklike crystals of **2** were obtained in 23% yield (based on P). Anal. Calcd for **2**: C, 2.70; H, 1.76; N, 2.88; Cu, 4.04; Na, 0.45; P, 1.21; W, 61.1. Found: C, 2.54; H, 1.65; N, 3.01; Cu, 3.89; Na, 0.58; P, 1.09; W, 60.7. IR (KBr pellet) $\bar{\nu}_{\max}$ (cm⁻¹): 2932 (w), 2280 (w), 1706 (w), 1645 (m), 1558 (m), 1078 (m), 941 (w), 901 (w), 785 (s), 678 (s), 579 (w).

Synthesis of Compound 3. K₁₂[H₂P₂W₁₂O₄₈]·~24H₂O (0.3 g, 0.076 mmol), 1 M CuCl₂ aqueous solution (0.75 mL, 0.75 mmol), hn (0.05 mL, 0.488 mmol), and NaCl (0.05 g, 0.86 mmol) were dissolved in 9 mL of distilled water. The mixture was stirred for 0.5 h and was transferred to a Teflon-lined stainless-steel autoclave (15 mL). The Teflon-lined stainless-steel autoclave was heated to 160 °C within 45 min, was kept at 160 °C for 15 days, and was then cooled to room temperature at a rate of 10 °C/h. Brown blocklike crystals of **3** were obtained from the solid product in 49% yield (based on P). Anal. Calcd for **3**: C, 3.71; H, 1.55; N, 1.44; Na, 1.42; Cu, 1.31; P, 1.27; W, 64.3. Found: C, 3.42; H, 1.71; N, 1.23; Na, 1.51; Cu, 1.41; P, 1.06; W, 63.8. IR (KBr pellet) $\bar{\nu}_{\max}$ (cm⁻¹): 3048 (w), 1704 (w), 1645 (w), 1559 (m), 1510 (m), 1078 (m), 938 (w), 785 (w), 673 (s), 519 (w).

X-ray Crystallography. The crystallographic data were performed on a Rigaku R-Axis RAPID IP diffractometer (for **1** and **3**) and a Bruker Apex CCD diffractometer (for **2**). In all cases, the data were collected at 150 K, and graphite-monochromated Mo K α radiation ($\lambda = 0.71073$ Å) was used. Multiscan absorption corrections were applied for compounds **1**, **2**, and **3**. The structures were solved by the direct method and were refined by full-matrix least-squares on *F*² using SHELXL-97 software.¹⁴ During the refinement of **1–3**, there was a number of short connections between OW_{water}···O_{POM} in the range of 2.60–2.90 Å, which suggests the extensive hydrogen bonding interactions between lattice water molecules and the POMs. However, the H atoms between them could not be determined from the difference Fourier maps because of the limited quality of the data. All hydrogen atoms on water molecules and protonated O atoms were directly included in the molecular formula. The H atoms on C and N atoms were situated in geometrically calculated positions. In **1–3**, only partial lattice water molecules can be accurately assigned from the residual electron peaks, whereas the rest were directly included in the molecular formula on the basis of the elemental analyses and thermogravimetric (TG) analyses. The crystal data and structure refinements of compounds **1**, **2**, and **3** are summarized in Table 1 (CSD reference no. 419042 for **1** and CCDC reference nos. 674716 and 674717 for **2** and **3**, respectively).

Results and Discussion

Synthesis. In this Article, the DDTP [α_1 -CuP₂W₁₇-O₆₀(OH)]₂¹⁴⁻ can be obtained not only by the conventional aqueous solution method but also by the hydrothermal technique with the mixture of the hexavacant Wells–Dawson-type polyoxoanion P₂W₁₂ and CuCl₂ in a NaCl aqueous solution. It is well known that the polyoxoanion P₂W₁₂ is very capable of combining metal cations and is a metastable precursor that could easily decompose in the aqueous

(14) (a) Sheldrick, G. M. *SHELXL97 Program for Crystal Structure Refinement*; University of Göttingen: Göttingen, Germany, 1997. (b) Sheldrick, G. M. *SHELXS97 Program for Crystal Structure Solution*; University of Göttingen: Göttingen, Germany, 1997.

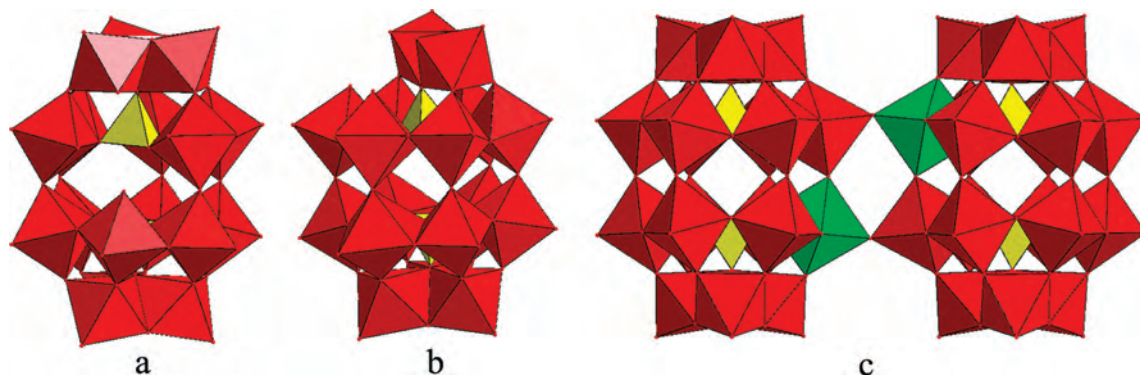


Figure 1. (a) Monovacant α_1 - P_2W_{17} unit obtained by removing a WO_6 octahedron in the equatorial site of the parent Wells–Dawson structure, (b) monovacant α_2 - P_2W_{17} unit obtained by removing a WO_6 octahedron in the capping region of the parent Wells–Dawson structure, and (c) a polyhedral representation of the DDTP in compound **1**. Tungsten, phosphorus, copper, and oxygen are colored red, yellow, green, and red, respectively.

solution.^{12,15} In this reaction, the WO_6 fragments arising from the (limited) decomposition of P_2W_{12} compete with the extra added Cu^{2+} ions, which has been observed in previous reports.^{15f,h} Additionally, the hydrothermal technique has been proven to be a powerful synthetic method in making new saturated POM-based hybrid compounds. Recently, a series of novel TM-substituted POMs (TMSPs) have been documented by virtue of this synthetic technique.¹⁶ It is found that most of these compounds are based on the classical trivalent or tetravalent Keggin building blocks. In our work, we attempt to prepare these TMSPs on the basis of the lacunary Dawson units, especially by the use of hexavacant Dawson anions as precursors.^{17,16f} Herein, we prepared two inorganic–organic hybrids based on the Cu-substituted Wells–Dawson units by carefully controlling the reaction conditions. During the synthesis, two types of organoamines were introduced into the reaction system. It is noteworthy that the number, size, and shape of organoamines play an obvious role in the final products.^{16a} In the preparation of compound **2**, if the amount of en (volume) is larger than 0.25 mL or if hn is absent, then no crystals can be isolated. However, if en is absent in the reaction system, then compound **3** can be obtained.

Structure Description. Single-crystal X-ray diffraction analyses confirm the presence of the monovacant $[\alpha_1-P_2W_{17}O_{61}]^{10-}$ (abbreviated as α_1 - P_2W_{17}) unit in the three compounds. Until now, two isomers of the monovacant derivatives of the Wells–Dawson anion have been observed in the literature. As shown in Figure 1a, the polyoxoanion α_1 - P_2W_{17} can be obtained by removing a WO_6 octahedron from the belt region of its parent Wells–Dawson structure $[\alpha-P_2W_{18}O_{62}]^{6-}$. This polyoxoanion has been reported several times in the Ln-containing polyoxoanion (monomer and dimer).¹⁸ However, in TMSP chemistry, the dimeric POMs containing the α_1 - P_2W_{17} have never been reported, and only a few monomers containing the α_1 - P_2W_{17} unit have been documented in the literature,¹⁹ such as the mono-TM-substituted α_1 -type Wells–Dawson compounds $[\alpha_1-K_8P_2W_{17}MO_{61}]$ ($M = Cu^{2+}, Mn^{2+}, Co^{2+}, Ni^{2+}, Zn^{2+}$) reported by Contant et al.^{19e} These compounds are obtained by the reaction of monovacant α_1 - $K_9LiP_2W_{17}O_{61} \cdot 18H_2O$ with the TM^{2+} cations and the 1-D linear chain structures $[Cu(en)_2(H_2O)]_2 - ([Cu(en)_2](\alpha_1-P_2W_{17}CuO_{61}))^{2-}$, $[(Cu(en)_2)_2P_2CuW_{17}O_{61}]^{6-}$,^{9a} and $(H_2en)_{0.5}H[Cu(en)_2(H_2O)]_2([Cu(en)_2](\alpha_1-P_2W_{17}CuO_{61}))$,^{11d} which were all constructed from the monocopper-substituted Dawson polyoxoanion. Figure 1b shows the α_2 -type monovacant Wells–Dawson anion that is obtained by the loss of a WO_6 octahedron in the capping region of the parent Wells–Dawson structure $[\alpha-P_2W_{18}O_{62}]^{6-}$, which has been commonly observed in POM chemistry.^{20,11e} The polyoxoanion in **1** was composed of two α_1 - P_2W_{17} units. Each half-unit contains a CuO_6

- (15) (a) Mal, S. S.; Dickman, M. H.; Kortz, U.; Todea, A. M.; Merca, A.; Bogge, H.; Glaser, T.; Müller, A.; Nellutla, S.; Kaur, N.; van Tol, J.; Dalal, N. S.; Keita, B.; Nadjo, L. *Chem.—Eur. J.* **2008**, *14*, 1186. (b) Contant, R. *Inorg. Synth.* **1990**, *27*, 104. (c) Müller, A.; Pope, M. T.; Todea, A. M.; Böge, H.; van Slageren, J.; Dressel, M.; Gouzerh, P.; Thouvenot, R.; Tsukerblat, B.; Bell, A. *Angew. Chem., Int. Ed.* **2007**, *46*, 4477. (d) Mal, S. S.; Kortz, U. *Angew. Chem., Int. Ed.* **2005**, *44*, 3777. (e) Pichon, C.; Mialane, P.; Dolbecq, A.; Marrot, J.; Rivière, E.; Keita, B.; Nadjo, L.; Sécheresse, F. *Inorg. Chem.* **2007**, *46*, 5292. (f) Zimmermann, M.; Belai, N.; Butcher, R. J.; Pope, M. T.; Chubarova, E. V.; Dickman, M. H.; Kortz, U. *Inorg. Chem.* **2007**, *46*, 1737. (g) Mal, S. S.; Nsouli, N. H.; Dickman, M. H.; Kortz, U. *Dalton Trans.* **2007**, 2627. (h) Godin, B.; Vaissermann, J.; Herson, P.; Ruhlmann, L.; Verdager, M.; Gouzerh, P. *Chem. Commun.* **2005**, 5624. (i) Godin, B.; Chen, Y.-G.; Vaissermann, J.; Ruhlmann, L.; Verdager, M.; Gouzerh, P. *Angew. Chem., Int. Ed.* **2005**, *44*, 3072. (j) Ostuni, A.; Pope, M. T. *C. R. Chim.* **2000**, *3*, 199.
- (16) (a) Zhao, J.-W.; Jia, H.-P.; Zhang, J.; Zheng, S.-T.; Yang, G.-Y. *Chem.—Eur. J.* **2007**, 10030. (b) Zheng, S.-T.; Yuan, D.-Q.; Zhang, J.; Yang, G.-Y. *Inorg. Chem.* **2007**, *46*, 4569. (c) Zhao, J.-W.; Zhang, J.; Zheng, S.-T.; Yang, G.-Y. *Inorg. Chem.* **2007**, *46*, 10944. (d) Wang, J. P.; Wang, W.; Niu, J. *Inorg. Chem. Commun.* **2007**, *10*, 1054. (e) Zheng, S.-T.; Wang, M.-H.; Yang, G.-Y. *Chem. Asian J.* **2007**, *2*, 1380. (f) Zhang, Z.; Liu, J.; Wang, E.; Qin, C.; Li, Y.; Qi, Y.; Wang, X. *Dalton Trans.* **2008**, 463.
- (17) Zhang, Z.-M.; Yao, S.; Li, Y.-G.; Wang, Y.-H.; Qi, Y.-F.; Wang, E.-B. *Chem. Commun.* **2008**, 1650.

- (18) (a) Luo, Q.-H.; Howell, R. C.; Dankova, M.; Bartis, J.; Williams, C. W.; Horrocks, W. D., Jr.; Young, V. G., Jr.; Rheingold, A. L.; Francesconi, L. C.; Antonio, M. R. *Inorg. Chem.* **2001**, *40*, 1894. (b) Sadakane, M.; Dickman, M. H.; Pope, M. T. *Inorg. Chem.* **2001**, *40*, 2715. (c) Boglio, C.; Lenoble, G.; Duhayon, C.; Hasenknopf, B.; Thouvenot, R.; Zhang, C.; Howell, R. C.; Burton-Pye, B. P.; Francesconi, L. C.; Lacôte, E.; Thorimbert, S.; Malacria, M.; Afonso, C.; Tabet, J.-C. *Inorg. Chem.* **2006**, *45*, 1389. (d) Huang, W.; Schopfer, M.; Zhang, C.; Howell, R. C.; Todaro, L.; Gee, B. A.; Francesconi, L. C.; Polenova, T. *J. Am. Chem. Soc.* **2008**, *130*, 481.
- (19) (a) Boglio, C.; Micoine, K.; Rémy, P.; Hasenknopf, B.; Thorimbert, S.; Lacôte, E.; Malacria, M.; Afonso, C.; Tabet, J.-C. *Chem.—Eur. J.* **2007**, *13*, 5426. (b) Bartis, J.; Kunina, Y.; Blumenstein, M.; Francesconi, L. C. *Inorg. Chem.* **1996**, *35*, 1497. (c) Contant, R.; Abbessi, M.; Canny, J.; Belhouari, A.; Keita, B.; Nadjo, L. *Inorg. Chem.* **1997**, *36*, 4961. (d) Micoine, K.; Hasenknopf, B.; Thorimbert, S.; Lacôte, E.; Malacria, M. *Org. Lett.* **2007**, *9*, 3981. (e) Contant, R.; Richet, M.; Lu, Y. W.; Keita, B.; Nadjo, L. *Eur. J. Inorg. Chem.* **2002**, 2587.

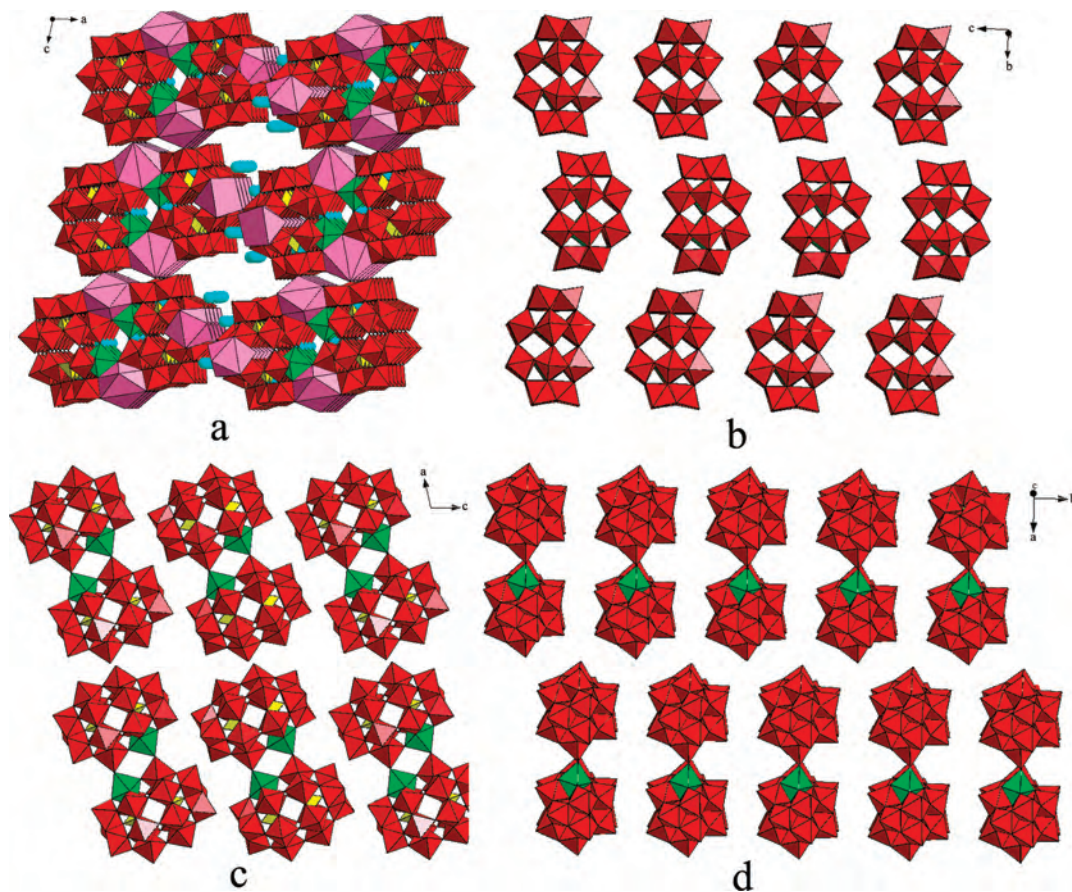


Figure 2. (a) Polyhedral and ball–stick representation of the 3-D structure of compound **1** linked by K^+ and Na^+ ions and a polyhedral representation of the packing arrangements of **1** viewed along different directions (b), (c), and (d). For clarity, K^+ , Na^+ , and the lattice water molecules are omitted. Tungsten, phosphorus, copper, sodium, potassium, and oxygen are colored red, yellow, green, blue, pink, and red, respectively.

octahedron at the belt region of the parent Wells–Dawson structure, and two half-units are fused together by two $W-OH-Cu$ groups to form a DDTP $[\alpha_1-CuP_2W_{17}O_{60}(OH)_2]^{14-}$ (Figure 1c). As we know, such a DDTP structure has been observed only once in a Fe-substituted polyoxoanion $[H_2P_4W_{28}Fe_8O_{120}]^{16-}$,^{15f} but it is structurally and compositionally different from the polyoxoanion in **1**. In the packing arrangement of **1**, all of the planes of these POMs are parallel to each other and are further connected by potassium and sodium cations in a 3-D framework. (See Figure 2.) Approximately 58 lattice water molecules reside in the interspaces of the crystal structure and are coordinated with alkali cations or are hydrogen bonded to the surface O atoms of the dimeric polyoxoanions.

Compound **2** exhibits a 2-D network that is composed of the DDTP $[\alpha_1-CuP_2W_{17}O_{60}(OH)_2]^{14-}$ and $[Cu(en)_2]^{2+}$ bridging units. In **2**, a $[Cu(7)(en)_2]^{2+}$ unit is sandwiched between two $\alpha_1-CuP_2W_{17}O_{61}(OH)$ monomers. The six-coordinate environment of this $Cu(7)^{2+}$ ion is completed by four N atoms of two en molecules and two O atoms derived from two $\alpha_1-CuP_2W_{17}O_{61}(OH)$ units (Figure 3). Furthermore, another seven $[Cu(en)_2]^{2+}$ groups are coordinated directly on the surface oxygen atoms of the dimeric polyoxoanion $(\alpha_1-CuP_2W_{17}O_{61}(OH)_2)^{14-}$, forming the first example of seven-supported DDTP. The seven $[Cu(en)_2]^{2+}$ units can be

divided into two groups according to their roles in the construction of the 2-D network. The first group is the $Cu(8)$ center, which is located at the pole site of DDTP and exhibits the octahedral coordination geometry with one bridging oxygen atom derived from the polyoxoanion ($Cu(8)-O(79) = 2.720(18) \text{ \AA}$), four nitrogen atoms originated from two en molecules (average bond length of $Cu(8)-N = 2.012 \text{ \AA}$), and one water molecule ($Cu(8)-O(1w) = 2.205(17) \text{ \AA}$). The second group contains the other six Cu centers. All of them possess the six-coordinate environment that is completed by four nitrogen atoms derived from two en molecules and two oxygen atoms originated from the dimeric polyoxoanion. In the six Cu^{2+} centers, the $Cu(6)$ and $Cu(6A)$ ions link the DDTP to constitute a 1-D zigzag polymer chain, as shown in Figure 4. These chains are further linked by the other four Cu^{2+} ions to form a 2-D network. It is noteworthy that there are two types of pores (A and B) in this 2-D network (see Figure 5a). Pore A is large enough to accommodate an hn molecule (Figure S1). We believe that the hn molecules serve as templates so that hybrid anionic building blocks are aggregated around them, leading to the assembly of a 2-D network.

These 2-D layers are further packed to form a 3-D supramolecular framework via extensive hydrogen bonding interactions between en molecules and DDTP (see Figures 5b and S5). The typical hydrogen bond distances are $N(13)\cdots O(108) = 2.976(26)$, $N(10)\cdots O(16) =$

(20) Fang, X.; Anderson, T. M.; Hou, Y.; Hill, C. L. *Chem. Commun.* **2005**, 5044.

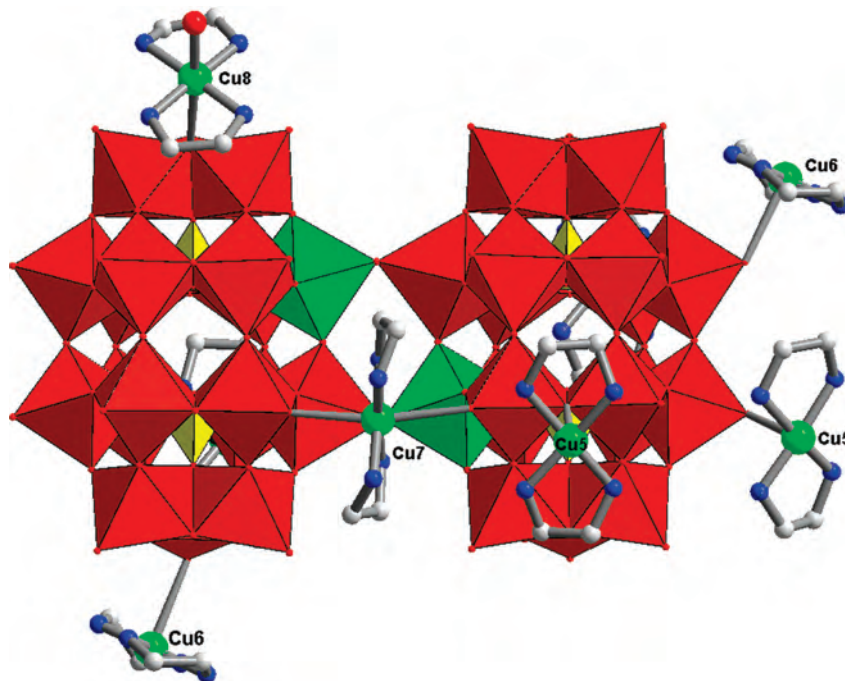


Figure 3. Polyhedral and ball–stick representation of the polyoxoanion of compound **2**. Tungsten, phosphorus, copper, oxygen, carbon, and nitrogen are colored red, yellow, green, red, light gray, and blue, respectively.

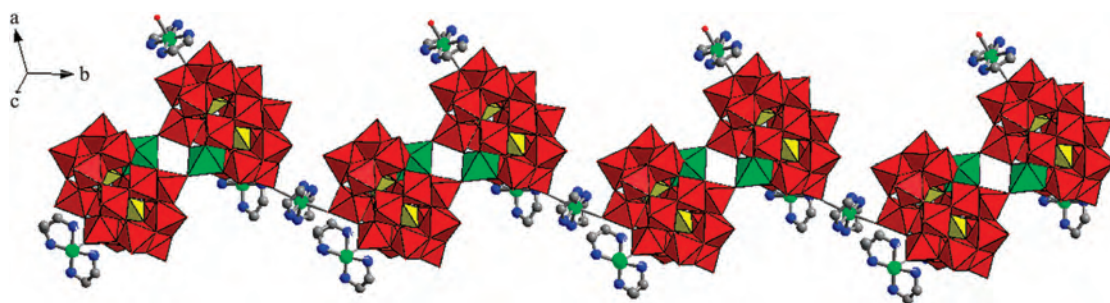


Figure 4. Polyhedral and ball–stick representation of the 1-D zigzag chain in compound **2**.

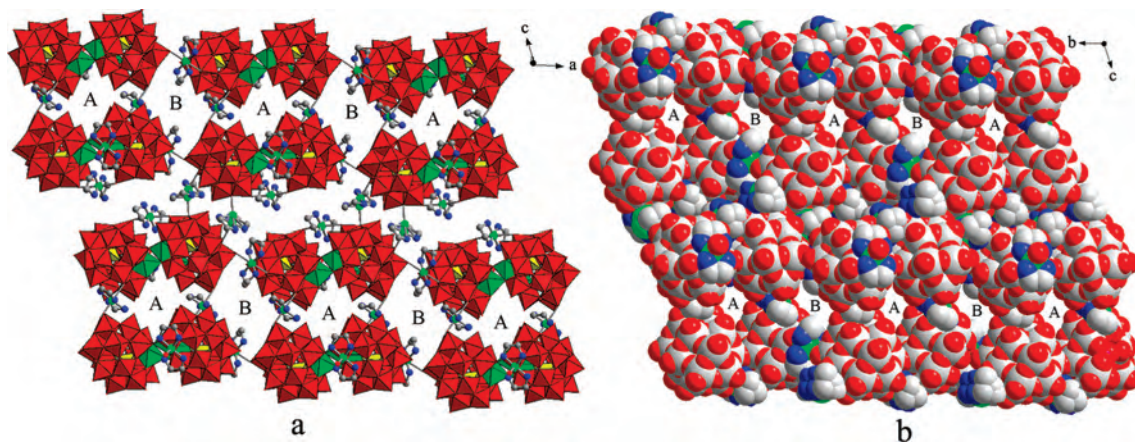


Figure 5. (a) Polyhedral and ball–stick representation of the 2-D framework structure of compound **2** and (b) space-filling diagrams of the 3-D supramolecular hybrid metal oxide of compound **2**. Tungsten, phosphorus, copper, oxygen, carbon, and nitrogen are colored red, yellow, green, red, light gray, and blue, respectively.

2.948(22), N(12)···O(16) = 2.907(28), N(21)···O(92) = 3.084(27), N(21)···O(77) = 2.986(29), and N(21)···O(46) = 3.100(26) Å. The long pores in two neighboring layers are well-overlapped so that the 3-D supramolecular framework exhibits two types of 1-D channels (A = 14.2 × 6.3 and B = 9.1 × 6.0 Å²). Channel A is occupied by

the dissociated hn molecules, whereas channel B is occupied by the lattice water molecules. To our knowledge, polyoxoanion (α_1 -CuP₂W₁₇O₆₁(OH))₂¹⁴⁻ in **2** is the current largest polyoxotungstate building block in the construction of extended organic–inorganic hybrid materials.

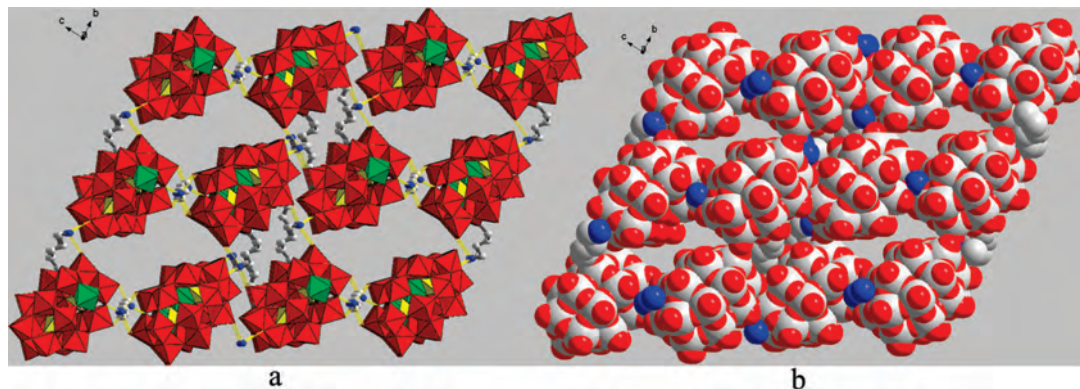


Figure 6. (a) Polyhedral and ball–stick representation of the 3-D supramolecular hybrid metal oxide with 1-D tunnels along the *a* axis in compound **3** and (b) space-filling diagrams of the 3-D supramolecular hybrid metal oxide with 1-D tunnels along the *a* axis in compound **3**. Tungsten, phosphorus, copper, oxygen, carbon, and nitrogen are colored red, yellow, green, red, light gray, and blue, respectively.

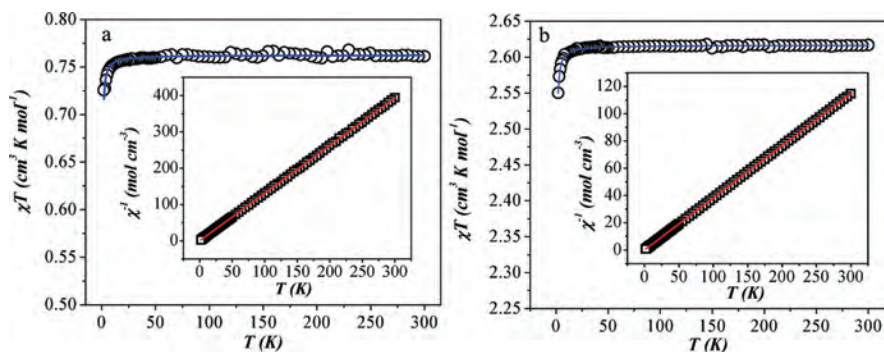


Figure 7. χT vs T and χ^{-1} vs T curves of compounds (a) **1** and (b) **2**.

Compound **3** consists of $[\alpha_1\text{-P}_2\text{W}_{17}\text{O}_{60}\text{Cu}(\text{OH})_2]^{8-}$, protonated hn molecules, sodium cations, and ca. 14 lattice water molecules. In **3**, the polyoxoanions $[\alpha_1\text{-P}_2\text{W}_{17}\text{O}_{60}\text{Cu}(\text{OH})_2]^{8-}$ are hydrogen bonded with hn molecules to form a 3-D supermolecular framework (Figure 6). The typical hydrogen bond distances are $\text{N}(4)\cdots\text{O}(40) = 2.9020(78)$, $\text{N}(4)\cdots\text{O}(63) = 2.835(63)$, $\text{N}(4)\cdots\text{O}(33) = 2.869(59)$, $\text{N}(1)\cdots\text{O}32 = 2.847(47)$, $\text{N}(1)\cdots\text{O}(37) = 2.956(68)$, and $\text{N}(1)\cdots\text{O}(21) = 3.010(57)$ Å. Interestingly, this 3-D framework possesses a 1-D channel along the *a* axis with dimensions of ca. 16.9×4.24 Å² (Figure 6b). The channels were filled with sodium cations and lattice water molecules.

In all three compounds, the Cu^{2+} centers and their neighboring W centers in the polyoxoanions exhibit a site-occupancy disorder (as shown in Figures S2–4). The oxidation states of W and Cu sites are determined on the basis of bond lengths and bond angles, the charge balance consideration, and bond valence sum calculations,²¹ indicating that all W and Cu sites possess +6 and +2 oxidation states, respectively. Bond valence sum calculations²¹ also reveal that the bridging oxygen atoms (O(11) in **1**; O(77) and O(56) in **2**) between Cu and W centers in the polyoxoanions of **1** and **2** and the terminal oxygen atom on W/Cu sites (O(50) and O(53)) in the polyoxoanion of **3** are monoprotonated (on the basis of the BVS value of O: H_2O , $V < 0.5$; OH, $0.5 < V < 1.5$; O^{2-} , $V > 1.5$).

(21) The valence sum calculations are performed on a bond valence calculator program, version 2.00, February 1993, written by C. Hormillosa with assistance from S. Healy and distributed by I. D. Brown.

Magnetic Properties. The solid-state magnetic behaviors of **1** and **2** have been investigated. The dc magnetic susceptibility (χ) data were measured in the temperature range of 2–300 K in a 0.1 T magnetic field and are plotted as χT and χ^{-1} versus T , as shown in Figure 7. The χT value of **1** slowly decreases from $0.76 \text{ cm}^3 \cdot \text{K} \cdot \text{mol}^{-1}$ at 300 K to $0.72 \text{ cm}^3 \cdot \text{K} \cdot \text{mol}^{-1}$ at 2 K, which reveals principally paramagnetic behavior (as shown in Figure 7a). The χT product at 300 K is slightly higher than the spin-only value ($g = 2.0$) of $0.75 \text{ cm}^3 \cdot \text{K} \cdot \text{mol}^{-1}$ for two noninteracting Cu^{2+} ions ($S = 1/2$). The χ^{-1} versus T plot is fitted by the Curie–Weiss law in the whole temperature range with $C = 0.75 \text{ cm}^3 \cdot \text{K} \cdot \text{mol}^{-1}$ and $\Theta = -0.09$ K. The small Weiss constant indicates that the magnetic interactions between Cu(II) ions are very weak. On the basis of the connection modes of Cu(II) ions in the polyoxoanion of **1**, the susceptibility was simulated by a dimeric Cu model with the isotropic Heisenberg spin Hamiltonian

$$H = -2JS_1S_2 \quad (1)$$

where S_i is the spin operator for each metal ion ($S_i = 1/2$ for Cu(II) with $i = 1$ to 2) and J is the magnetic interaction between the two central Cu(II) sites. The magnetic data of **1** are fitted to the following equation where N , g , μ_B , and k_B have their usual meanings

$$\chi_{\text{dimer}} = \frac{2Ng^2\mu_B^2}{k_B T} \frac{1}{3 + e^{-2J/k_B T}} \quad (2)$$

This simulation procedure works well in the whole temperature range (see the blue line in Figure 7a) with the

parameters $g = 2.02$ and $J/k_B = -0.23$ K. The small J/k_B value further confirms that there is only a very weak antiferromagnetic interaction between Cu(II) centers.

The χT vs T plot of **2** exhibits behavior similar to that of **1**. The χT product of $2.62 \text{ cm}^3 \cdot \text{K} \cdot \text{mol}^{-1}$ at 300 K is a little higher than the spin-only value ($g = 2.0$) of $2.44 \text{ cm}^3 \cdot \text{K} \cdot \text{mol}^{-1}$ for 6.5 noninteracting Cu^{2+} ions ($S = 1/2$). The χ^{-1} vs T plot agrees with the Curie–Weiss law in the whole temperature range with $C = 2.61 \text{ cm}^3 \cdot \text{K} \cdot \text{mol}^{-1}$ and $\Theta = -0.05$ K. (See the black line in Figure 7b.) Furthermore, the susceptibility data of **2** are simulated with the following equation

$$\chi = \chi_{\text{dimer}} + 4.5Ng^2\mu_B^2S(S+1)/3k_B T \quad (3)$$

where the first term refers to the susceptibility of the dimeric Cu unit in the polyoxoanion of **2**, the second term refers to that of the Curie contribution for the 4.5 isolated Cu(II) metal ions ($S = 1/2$), and N , g , μ_B , and k_B have their usual meanings. The fit works well in the whole temperature range (see the blue line in Figure 7b) with the parameters: $g = 2.02$ and $J/k_B = -0.31$ K. The small J/k_B value indicates that there is only a very weak antiferromagnetic interaction between two Cu(II) ions in the dimeric polyoxoanion. The paramagnetic behaviors of **1** and **2** are consistent with their structures in which the Cu(II) centers are well separated.

Thermal Analyses. To examine the thermal stability of compounds **1**, **2**, and **3**, TG analyses were carried out for the three compounds. The TG curve of **1** shows a total weight loss of 10.5% in the range of 45–330 °C (calcd 10.6%), which corresponds to the loss of all noncoordinated and coordinated water molecules (Figure S9).

The TG curve of **2** (Figure S10) shows two weight-loss steps from 40 to 562 °C. The first weight loss of 8.80% in the temperature range of 40–235 °C corresponds to the release of lattice and coordinated water molecules, hn molecules, and noncoordinated en molecules. The second weight loss of 5.25% is attributed to the loss of all of the coordinated en molecules. The whole weight loss of 14.1% agrees with the calculated value of 14.0%. Compound **2** does not lose weight at temperatures that are higher than 562 °C.

The TG curve of **3** shows two continuous weight-loss steps from 30 to 281 °C (Figure S11). The whole weight loss of 11.4% corresponds to the loss of all lattice water molecules and noncoordinated hn ligands (calcd 11.3%).

Conclusions

Three $[\alpha_1\text{-CuP}_2\text{W}_{17}]$ -based POMs and their organic–inorganic hybrid compounds have been successfully synthesized. Compound **1** contains a DDTP that is composed of two $\alpha_1\text{-CuP}_2\text{W}_{17}\text{O}_{61}(\text{OH})$ anions that exhibit a new dimeric Dawson-type structure in POM chemistry. Compound **2** possesses a 2-D network constructed from the DDTP ($\alpha_1\text{-CuP}_2\text{W}_{17}\text{O}_{61}(\text{OH})_2^{14-}$ and $(\text{Cu}(\text{en})_2)^{2+}$ bridging units, representing the current largest polyoxotungstate building blocks in the construction of extended organic–inorganic hybrid materials. Compound **3** displays a 3-D supramolecular framework with 1-D tunnels based on the $[\alpha_1\text{-CuP}_2\text{W}_{17}]$ cluster and the protonated H_2hn organic cations. The magnetic studies of compounds **1** and **2** indicate that weak antiferromagnetic interactions exist in these two compounds and that the Cu(II) centers in the two compounds are well separated. Further research will focus on the synthesis of organic–inorganic hybrid materials based on other huge TM-substituted polyoxoanions so as to obtain the high-dimensional porous materials with magnetically and electrochemically active metal centers. This research is currently happening in our group.

Acknowledgment. This work was supported by the National Natural Science Foundation of China (no. 20701005), the Science and Technology Development Project Foundation of Jilin Province (no. 20060420), and the Postdoctoral Station Foundation of Ministry of Education (no. 20060200002).

Supporting Information Available: X-ray crystallographic data, TG curves, IR spectra, and additional Figures for compounds **1**, **2**, and **3**. This material is available free of charge via the Internet at <http://pubs.acs.org>.

IC800479K